JOURNAL OF MATERIALS SCIENCE 20 (1985) 3853–3864

Polarized infrared reflection spectroscopy of single crystal lithia-silicates and quartz

W. J. McCRACKEN
Metallurgy and Ceramics Laboratory, General Electric Company, St Petersburg, Florida 33733, USA

W. B. PERSON
Chemistry Department, University of Florida, Gainesville, Florida 32611, USA

L. L. HENCH
Materials Science and Engineering Department, University of Florida, Gainesville, Florida 32611, USA

The structures of single crystal lithia-silicate and quartz are characterized by polarized infrared reflection spectroscopy (PIRRS). The experimental apparatus and technique for PIRRS, along with electron channelling of lithia-disilicate, are discussed. Vibrational assignments are made for infrared reflection peaks of lithia-disilicate crystals and lithia-metasilicate crystals.

1. Introduction

The application of infrared spectroscopy to the identification and characterization of unknown organic compounds is well established and widely used. Infrared spectra of organic compounds generally exhibit sharp well-defined peaks that are assignable to the vibrations of the individual functional groups of which the molecule is comprised. However, the infrared spectra derived from silicate compounds usually have peaks that are broad and overlapping, making assignments and specific identification more difficult.

The frequencies at which a material absorbs (or reflects) infrared energy depend upon the internal vibrations of atoms in the molecule and hence its composition. Most infrared studies of silicates assume that the structural unit is a single Si–O tetrahedron with zero, one, or two nonbridging oxygens per tetrahedron which correlate with the symmetry point groups of T_d, C_{3v}, and C_{2v} respectively [1–12]. Sanders *et al.* related the frequency assignments to the possible vibrational modes for these single tetrahedral models [8]. When using infrared reflection spectroscopy, these assignments have been useful in characterizing glass structure and structural changes associated with glass corrosion [13–17]. In crystalline silicates, the ordering of the tetrahedra gives rise to additional peaks not predicted by a single Si–O tetrahedron model. Thus, to select the vibrational modes that correlate with the peaks in the infrared spectra of crystalline silicate solids, one must use a multi-unit (multi-tetrahedron) model as suggested by Gordon [18].

Infrared reflection methods of analysis of crystalline solids have been employed since the late 1930s by Matossi and co-workers [1, 19, 20]. The incident radiation sets the atoms of the material into oscillation and the reflected beam can be described as reradiation of this excitation. The spectra for silicates generated by reflection are generally different from the absorption spectra in that the optical constants (reflectance, η, and absorbance, k) of the material cause shifts of the reflection peaks from the characteristic absorption peaks. Thus the positions of peaks in the reflection spectra cannot be directly compared with either the absorption peak locations or the corrected (calculated) spectra from reflection data. An example of these differences and

0022–2461/85 $03.00 + .12

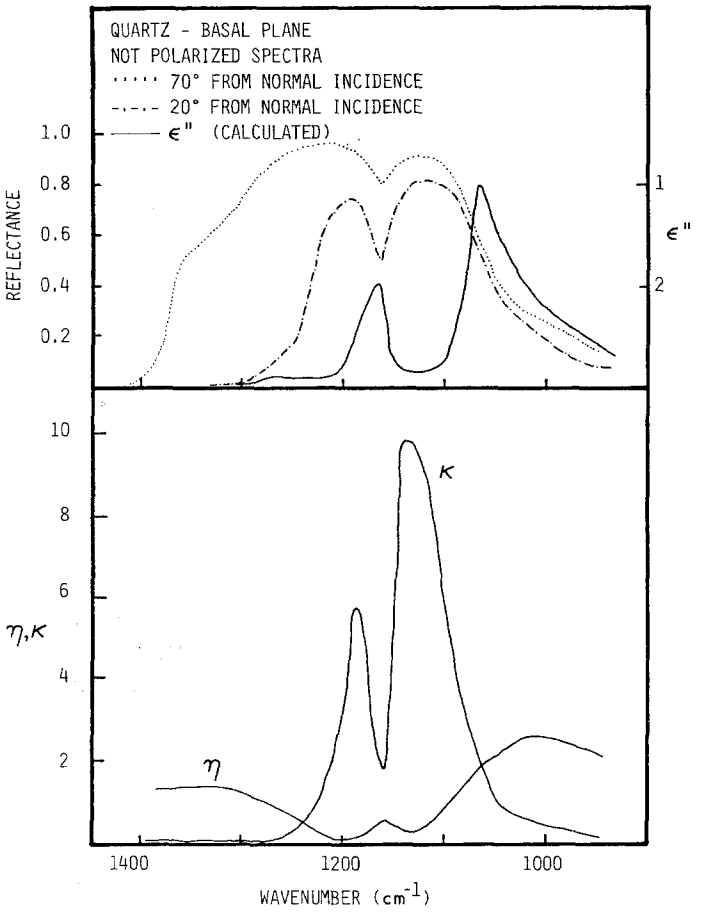

Figure 1 Infrared reflection spectra of quartz from two different angles of incidence (20° and 70°) and calculated optical constants η and k. Corrected spectrum (ε'') shows difference between reflection spectrum and absorption spectrum (after Simon and McMahon).

the effect of η and k are shown in Fig. 1 for quartz. A complete discussion of the correlations between reflection spectra and absorption spectra can be found in [11] and [21].

Reflection of infrared radiation from dielectric materials, such as silicates, generally produces partially plane-polarized light [22]. Near normal incidence reflection allows infrared sampling of approximately 0.5 μm into the surface of the silicate material [23, 24].

The absorption (or reflection) of electromagnetic radiation by a crystalline solid produces an oscillating electric moment associated with a given fundamental mode of vibration. In electromagnetic radiation that is plane-polarized, the electric field and the magnetic field are perpendicular. The oscillating electric moment can only interact with electromagnetic radiation that has its electric field in the same direction. Thus, the orientation of the fundamental mode of vibration can be determined by using plane-polarized radiation for either single crystals or oriented polycrystalline surfaces.

Polarized infrared radiation was used to examine the structure of several organic crystals as early as the 1930s [25]. The advantage of using polarized infrared reflection spectroscopy (PIRRS) is two-fold. Firstly, by identifying the characteristic vibrational direction for a given reflection peak, the mode of molecular vibration can be determined for the given crystal structure. When the crystallographic orientation of the crystal is known, the direction of vibration of the molecules in the incident plane that causes the reflection peaks must agree with the predicted direction in order for the assignment to be correct. Secondly, when spectral peaks overlap, making them difficult to identify, the PIRRS technique is a powerful method that can help to separate the observed peaks without the need for complex mathematical deconvolution techniques using computers. Each infrared peak can be characterized according to its symmetry in the crystal structure.

Peaks of different symmetry lying close together can be distinguished by analysing the

infrared radiation using a rotating polarizing filter at two different positions 90° apart. In an ideal case, the polarizer in one position would eliminate one of the peaks from the spectrum, allowing clear identification of the other peak. When the polarizer is rotated to the second position, the former peak may be identified.

For many crystals, the directions of the polarization axes are fixed by symmetry and become independent of the frequency of light. In uniaxial crystals of the hexagonal, trigonal, and tetragonal systems, and in biaxial crystals of the orthorhombic system, all the polarization axes are fixed by symmetry along the crystallographic axes.

For monoclinic crystals, one axis is fixed by symmetry, while the other two are unrestricted. Thus the spectra observed parallel or perpendicular to polarization axes are fixed by symmetry. These axes will assume a fundamental significance, while spectra taken in other directions can lead to erroneous interpretations.

The single crystal silicates used for this polarized infrared reflection spectroscopy study were quartz, SiO_2 (with almost symmetrical SiO_4 tetrahedra and zero nonbridging oxygen); lithia-silicate, $Li_2Si_2O_5$ (with a single nonbridging oxygen per tetrahedron); and lithia-metasilicate, Li_2SiO_3 (with two nonbridging oxygens per tetrahedron).

The crystal structure of quartz, which is based on a hexagonal lattice, was first determined by Gibbs [26]. The atomic arrangement for SiO_2 as given by Gibbs is as follows:

"The Si atoms are in four-coordination with oxygen, and constitute the (SiO_4) tetrahedron found as the basis unit of structure in all the known polymorphs of SiO_2 and in silicates in general. In quartz, each oxygen is shared with two Si atoms, the (SiO_4) tetrahedra thus being linked by sharing of each of the corner oxygen atoms to form a three-dimensional network. . . .

The (SiO_4) tetrahedron in quartz is almost symmetrical, with an Si–O distance of 1.61 Å. Each oxygen has, in addition to two Si atoms, six adjacent oxygen atoms at distances ranging between 2.60 and 2.67 Å. The Si–O bond is of intermediate type, roughly half covalent and half ionic [27]".

The significance of this structure lies in the fact that the SiO_4 tetrahedra have a T_d symmetry

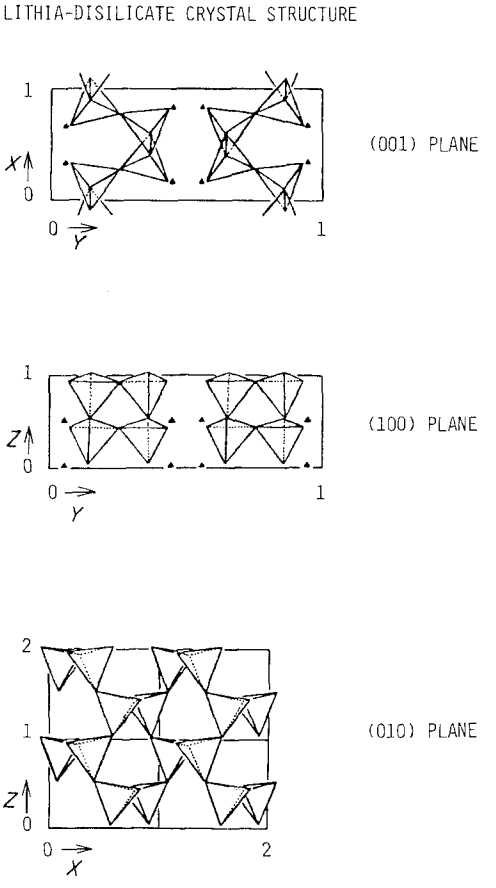

Figure 2 Crystal structure projections of the (0 0 1), (1 0 0) and (0 1 0) planes for lithia-disilicate ($Li_2Si_2O_5$) after Liebau.

point group because each of the oxygen atoms are bonded to two Si atoms.

The schematic projection after Liebau [28] in Fig. 2 shows that the structure of lithia-disilicate consists of SiO_4^{-4} tetrahedra linked together by three oxygen atoms. The fourth oxygen atom is bonded to a lithium atom and is not shared by the tetrahedra. This configuration gives lithia-disilicate a C_{3v} symmetry point group. The low-temperature form of $Li_2Si_2O_5$ is monoclinic with four formula units in the unit cell [28]. However, lithia-disilicate appears to be orthorhombic with three cleavages at right angles [29]. One cleavage parallel to the (0 1 0) plane is micaceous, the other two are nearly perfect. It should be noted that some current references still list $Li_2Si_2O_5$ as being orthorhombic.

The crystal structure of lithia-metasilicate contains two oxygen atoms per tetrahedron bonded to lithium atoms as shown in Fig. 3. Donnay and Donnay [30] describe the Li_2SiO_3

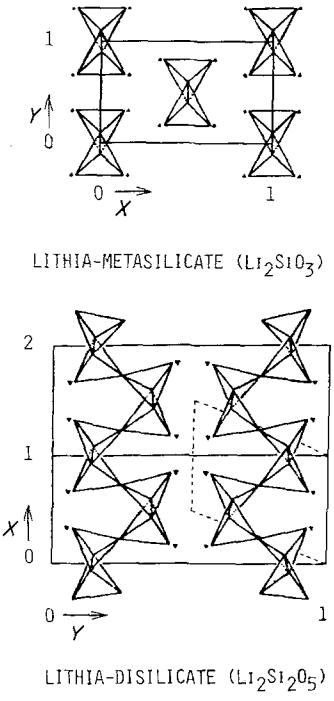

Figure 3 The crystal structure projections of the (0 0 1) plane for lithia-metasilicate (Li_2SiO_3) and lithia-disilicate ($Li_2Si_2O_5$).

structure as follows:

"It consists of single chains of SiO_4 tetrahedra, parallel to the *C* axis and held together by lithium atoms.The structure differs from that of the pyroxenes in that it has four alkali ions per Si_2O_6 link of the chain rather than two alkaline earth ions. With four lithium–oxygen bonds of strength 1/4, the Pauling rule is perfectly satisfied since each unshared oxygen receives four such bonds. The coordination polyhedron of lithium roughly approximates a tetrahedron."

Li_2SiO_3 exists in one form with an orthorhombic pseudo-hexagonal crystal structure.

There are three steps in the PIRRS method in order to determine the Si–O stretching peaks and also to assign the vibrational modes for single crystal silicates. First, determine the crystallographic orientation of the sample with respect to the infrared beam. The orientation of many single crystals can be determined visually, but some require microscopic or X-ray techniques. Second, determine the possible modes of infrared stretching vibrations in the crystal unit cell. Third, coordinate the polarized infrared reflection spectra obtained from the sample surface with the possible vibrational modes in the incident crystallographic plane.

2. Experimental details

2.1. Apparatus

The standard infrared reflection spectroscopic technique that has been used previously [8, 13–17] utilizes a dual beam Perkin-Elmer Model 467 grating spectrophotometer with a combination beam condenser-specular reflectance accessory Model 186-0373. This accessory is added to both the sample and the reference beam. For PIRRS, the accessory was added to the sample beam only with a venetian blind reference beam attenuator in order to adjust the baseline. The reference beam attenuator allowed for compensation of the AgBr polarizer element in the Perkin-Elmer wire grid polarizer accessory Model 186-1243 in the sample beam. This polarizing filter was selected for its extended spectral range (4000–250 cm^{-1}) [31] which is required for use with silicates (1300–250 cm^{-1}). Either the polarizer or the sample may be rotated. To minimize the polarization effects of the grating prism dispersion elements and to produce a flatter baseline as shown in Fig. 4, the polarizer was oriented at 45° (or 315°) with respect to the entrance slits of the spectrophotometer.

The orientation of the sample stage with respect to sample space polarizer was determined using an additional polarizing grid placed on the sample stage beneath a mirror.

With the sample space polarizer set at 45°, the polarizer on the stage was rotated to produce maximum transmittance as detected by the spectrophotometer. This located the position on the sample stage which correlates to 45° on the sample space polarizer. Two spectra were taken, one each with the polarizer at 45° and 315°, giving maximum difference in sample polarization effects, as shown in Figs. 5 and 6.

2.2. Sample preparation

PIRRS studies require the use of either single crystal samples or highly oriented samples. A 10.1 cm long, doubly ended single crystal of quartz provided an excellent sample. However, the lithia-disilicate (33L) and lithia-metasilicate (50L) samples had to be made. Glasses were prepared of each composition, using reagent grade materials, by melting them in a covered platinum crucible in a SiC glo-bar furnace at

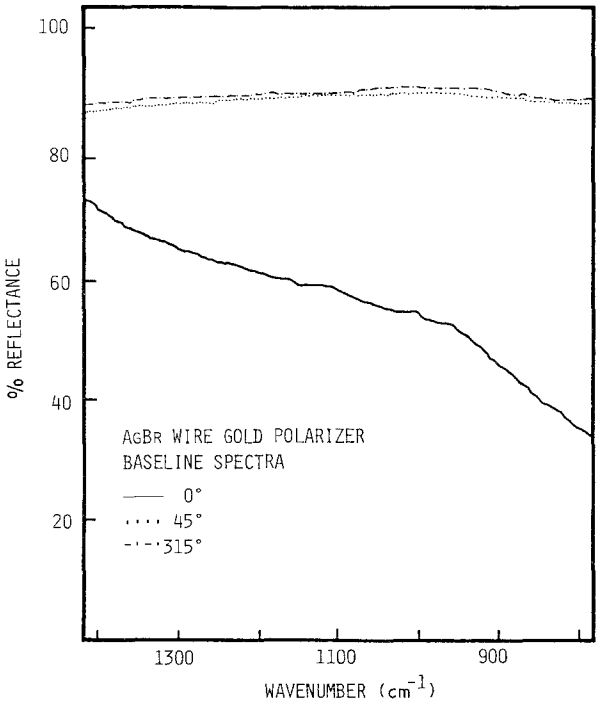

Figure 4 Polarized infrared reflection spectra of the AgBr wire grid polarizing filter showing the effect of polarizer orientation on the baseline intensity.

1350° C until homogenized (approximately 12 h). Each glass was then poured into an alumina crucible and returned to the furnace to reheat to 1350° C. Then the glasses were furnace cooled slowly (6 to 8 h) to room temperature. The resultant microstructure of each solid was comprised of large crystals. The samples were cut with a diamond wafering saw and polished with SiC paper.

The crystallographic orientation of the samples was accomplished by visual inspection and electron beam channelling. The sides of the quartz sample yielded the hexagonal prism face (1 0 $\bar{1}$ 0). The micaceous cleavage direction of the 33L crystals yielded the (0 1 0) plane. The (0 0 1) plane of the 33L crystal was obtained by cutting perpendicular to the micaceous layer and confirmed by electron channelling, Figs. 7 and 8. The 50L sample crystallized from the outside surface towards the centre, producing crystals with their growth axes (0 0 1) near parallel and their (1 0 0) axes and (0 1 0) axes random.

Electron beam channelling is a scanning electron microscopic technique which gives the crystallographic nature of the specimen. A detailed discussion of this technique can be found in [32] and [33]. The electron channelling pattern (ECP), Fig. 7b, is a reciprocal space

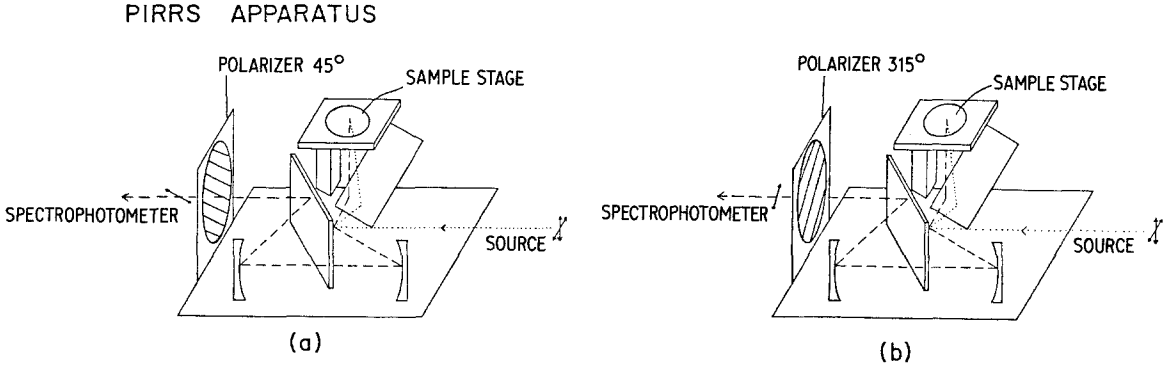

Figure 5 Reflectance-condenser apparatus with polarizing filter as used in the reference beam path of the spectrophotometer for PIRRS. Illustrates rotation of the polarizer to give two spectra 90° apart at 45° (a) and 315° (b).

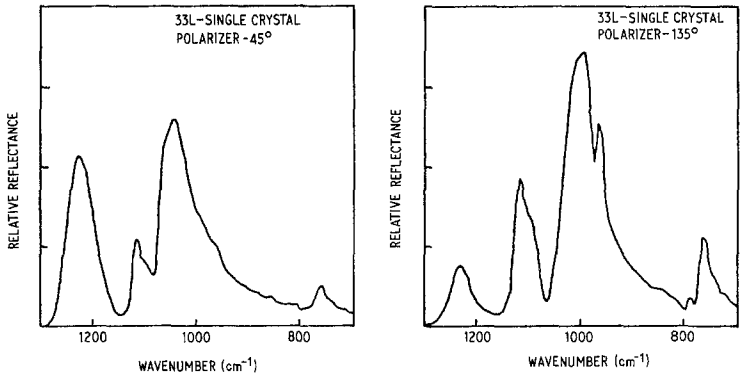

Figure 6 Polarized infrared reflection spectra obtained from the (0 0 1) plane of lithia-disilicate single crystal showing the change in spectra with rotation of the polarizer.

image (similar to a Kikuchi pattern) of the crystallographic planes of the specimen. The identification of the planes was done using the band widths and the interplanar angles. The band widths are inversely proportional to the plane spacing. The indexing of the ECP for a lithia-disilicate crystal is shown in Fig. 8. The (0 1 0) pole of the channelling pattern indicates the surface of the crystal is the (0 1 0) plane. Also from Fig. 7, the cleavage planes of the crystal are parallel to the (4 0 0) plane and the (0 0 2) plane in the ECP.

After the crystallographic plane of the sample surface was determined, the axes of that plane were determined by rotating the sample on the stage of the PIRRS apparatus in order to maximize the difference between the 45° spectra and the 315° spectra. This change in peak intensity in relation to the position of the polarizer is referred to as dichroism [34]. The ratio of the peak intensity when the electric field in the radiation is falling on the sample oriented in such a direction as to give maximum intensity, to the peak intensity when the electric field is perpendicular to this direction, is called the dichroic ratio. The experimentally determined dichroic ratios may differ from the sample material's actual ratio, giving rise to possible errors in the polarized infrared reflection spectra. Various reasons for such a difference are: imperfectly oriented samples, imperfect polarization by the polarizer, inherent polarization by the spectrophotometer, birefringence, and the effects of beam convergence in condensing systems [35].

3. Results and discussion

The infrared reflection spectrum of quartz has been the subject of various investigations [3, 5, 9], some using analysis by polarizers [11]. The results of this study using quartz are in Fig. 9.

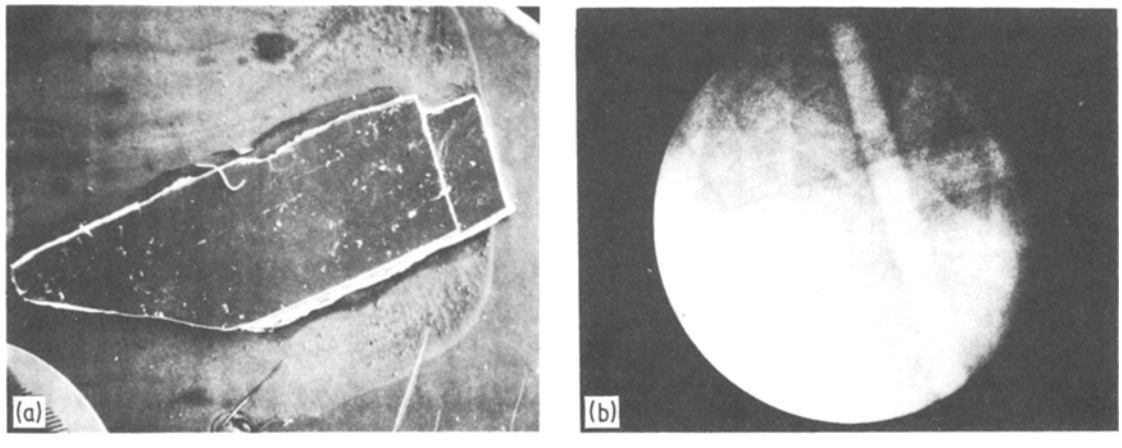

Figure 7 Lithium disilicate single crystal images from scanning electron microscope (a) secondary electron imaging mode (× 20) and (b) backscattered electron channelling mode.

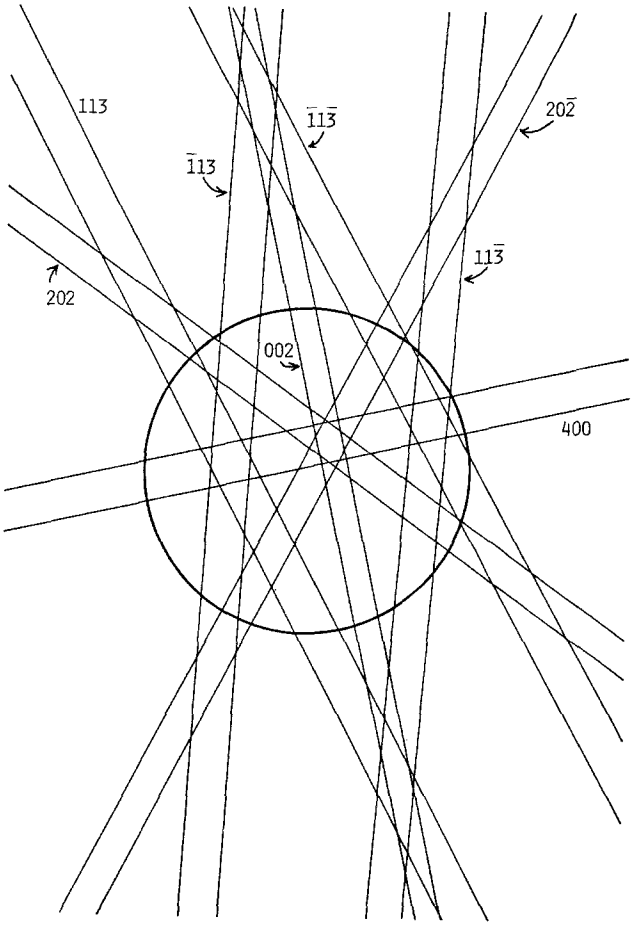

Figure 8 Diagram of the bands from the ECP of lithia-disilicate. The band inside the circle represents the electron channelling pattern in Fig. 7.

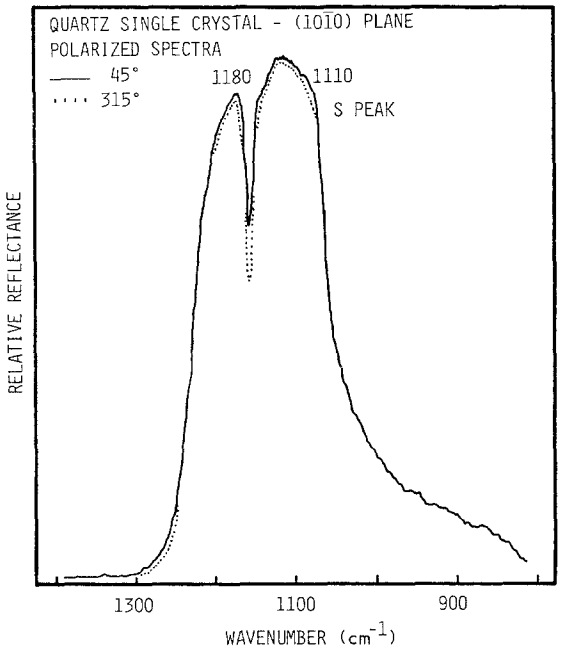

Figure 9 Polarized infrared reflection spectra of a quartz single crystal on the prism face (1 0 $\bar{1}$ 0).

The spectra were taken from a prism face parallel to the optic axis (0 0 0 1). The two PIRRS spectra were taken at 90° to each other showing no relative polarization.

Comparing the reflection data in Fig. 1 (after Simon [21]) and Fig. 9 shows similar spectra with two peaks at 1180 and 1110 cm^{-1}. As a result of the difference between reflection spectra and absorption spectra, Simon [21] warns that the dip (1160 cm^{-1}) in the broad reflection peak cannot be considered as a gap between two partially overlapping peaks, but rather a display of an individual, sharp absorption band. The peak at approximately 1110 cm^{-1} can be assigned to Si → O → Si vibration from a single SiO_4 tetrahedron with the symmetry point group T_d. This peak and peaks in other silicates from similar stretching vibrations will be referred to, in this work, as S peaks. These results agree with the assignment proposed for a vitreous SiO_4 tetrahedron in perfectly symmetrical conditions [8].

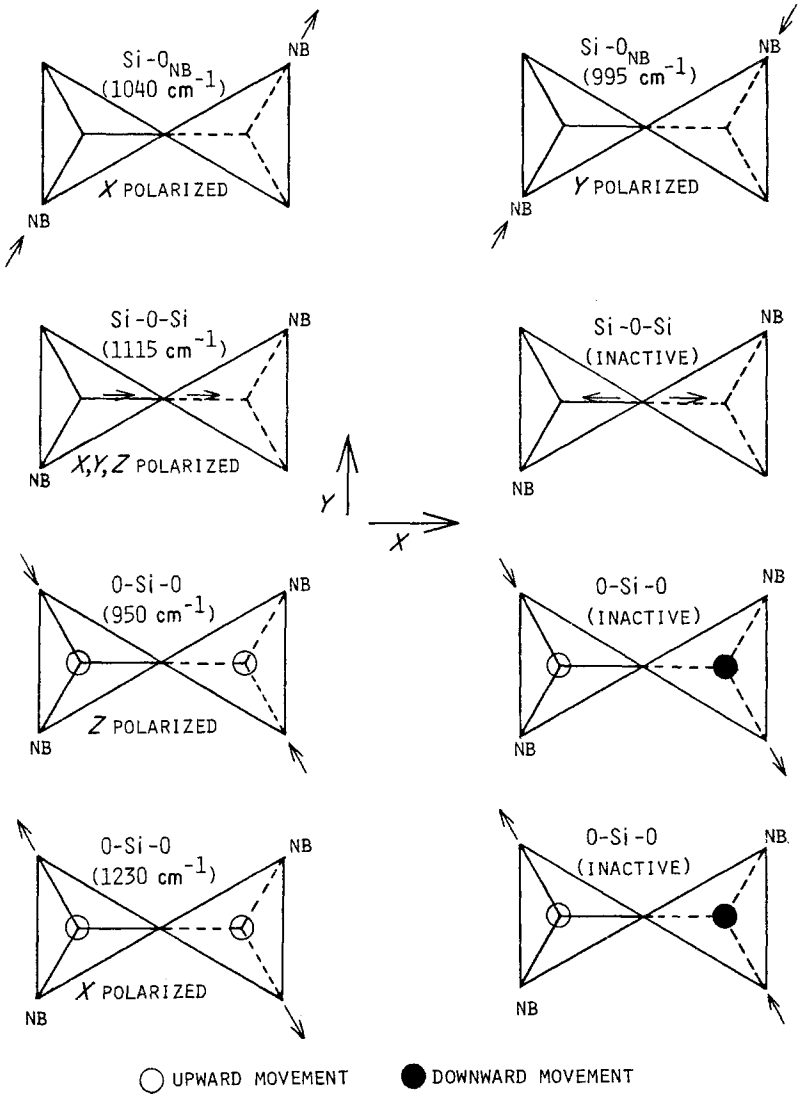

Figure 10 Oxygen tetrahedra for $Si_2O_7^{-2}$ unit with one nonbridging oxygen per tetrahedron illustrating possible Si–O bond stretching vibrational modes.

The peak at 1180 cm^{-1} can be assigned to the Si–O–Si stretching vibration between adjacent tetrahedra in the crystal structure. This vibration from the lattice structure gives an indication of the long-range order of the single tetrahedral units in silicates [9]. The basic unit cell used for predicting the possible modes of stretching vibration for lithia-disilicate is $Si_2O_7^{-2}$. This unit cell contains two oxygen tetrahedra with one nonbridging oxygen each, both of which are joined together by a point. Fig. 10 shows the unit cell with the eight possible stretching modes for the Si–O bonds. The unit cells are shown oriented with the primary axes with the characteristic polarization direction indicated.

For a more precise orientation of the unit cell with respect to the crystal structure, refer to Fig. 3. The frequency assignments were made after analysis of the PIRRS data from the two mutually perpendicular planes (0 1 0) and (0 0 1), as shown in Figs. 11 and 12, respectively. The one peak at 1115 cm^{-1} (an S peak) in all the spectra is the Si → O → Si stretching vibration that was predicted to have components in all directions in the crystal. From the spectra along the *X* direction in both of the planes, two peaks, 1230 and

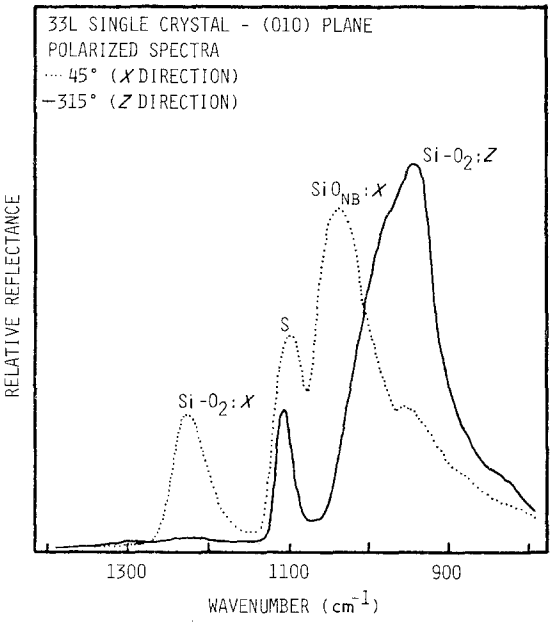

Figure 11 Polarized infrared reflection spectra of a lithia-disilicate single crystal on the (0 1 0) plane.

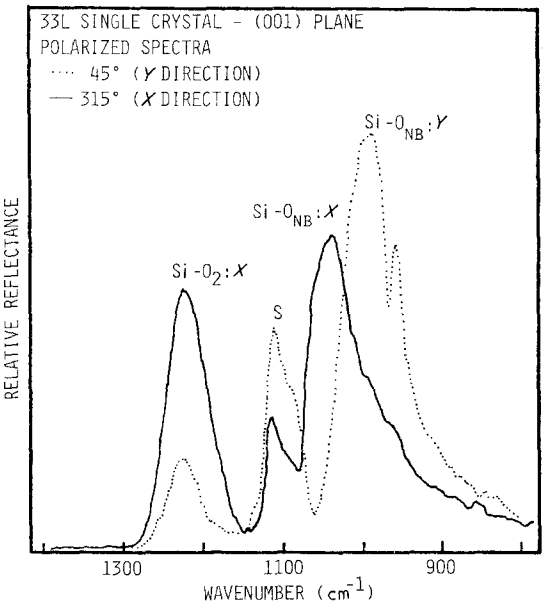

Figure 12 Polarized infrared reflection spectra of lithia-disilicate single crystal on the (0 0 1) plane.

1040 cm^{-1} are obtained in addition to the S peak. The predicted stretching vibrations are the silicon–nonbridging oxygen along the X direction (Si–O_{NB}:X) and the oxygen–silicon–oxygen along the X direction (Si–O_2:X). The silicon–nonbridging oxygen vibrational frequency has been shown to be lower than the S vibrational frequency [8, 9]. The peak assignment of 1040 cm^{-1} to Si–O_{NB}:X and 1230 cm^{-1} to Si–O_2;X therefore follows. Along the Z direction in Fig. 11, the only peak, besides the S, is at 950 cm^{-1} and is assigned to oxygen–silicon–oxygen vibration along the Z direction (Si–O_2:Z). Finally, the Y direction peaks at 995 cm^{-1} and 1230 cm^{-1} may be due either to imperfect crystal orientation in the infrared beam or to the stretching vibrational mode polarization direction that is not perfectly aligned with the crystal axis.

The $Si_2O_7^{-2}$ unit cell with two nonbridging oxygens per tetrahedron was used to predict the possible modes of vibration for lithia-metasilicate. Fig. 13 shows the predicted vibrational modes and polarization directions for infrared active Si–O stretching modes. The lithia-metasilicate samples contained long single crystals oriented with their axis of growth (0 0 1 or Z axis) parallel. Since these crystals are chain-like, the orientation of the X and Y direction was random. The PIRRS data for lithia-metasilicate (50L) taken from planes parallel to the Z axis and perpendicular to the Z axis are shown in Figs. 14 and 15, respectively. The spectra taken along the Z axis in Fig. 14 show two peaks at 870 and 1000 cm^{-1}. The 870 cm^{-1} peak is due to the O–Si–O stretching vibration (Si–O_2:Z) along the tetrahedral chains of the 50L structure. Radiation in the Z direction would more likely excite this vibrational mode than the vibrational modes of the Y direction. The two remaining peaks, 1120 and 965 cm^{-1}, are due to the Si–O–Si stretching (S:Y), which is polarized in this silicate, and the other silicon–nonbridging oxygen vibration [Si–$(O_{NB})_2$:Y], respectively. The S:Y peak is polarized, apparently due to the increase in symmetry of the SiO_4^{-4} tetrahedral positions in the metasilicate chain structure. The PIRRS data in Fig. 15 show that, perpendicular to the crystal growth direction, the structure has a random orientation about the Z axis.

4. Conclusions

The polarized infrared reflection spectroscopic technique is very useful in making vibrational mode assignments to spectral reflection peaks from single crystal silicates. Table I lists the spectral peaks for quartz, lithia-disilicate, and lithia-metasilicate. From this summary it can be

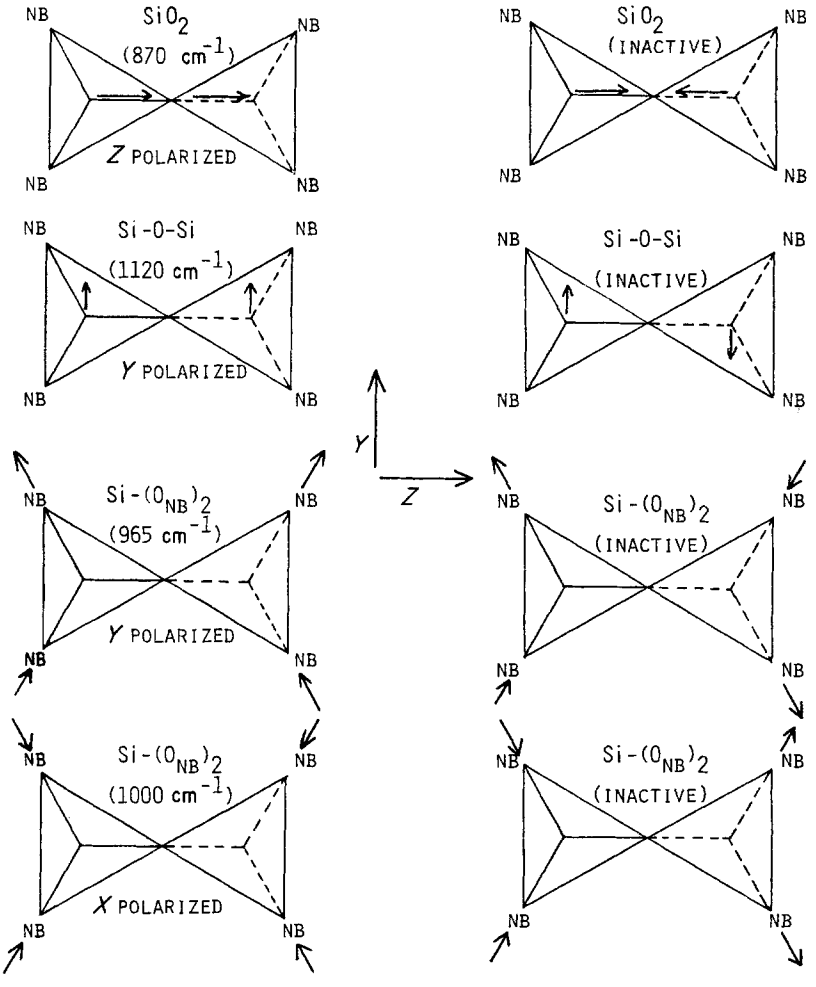

Figure 13 Oxygen tetrahedra for $Si_2O_7^{-2}$ unit with the two nonbridging oxygens per tetrahedron illustrating possible Si–O bond stretching infrared vibrational modes.

TABLE I Vibrational frequencies of infrared spectral peaks in the range 1400 to 800 cm^{-1} for quartz, lithia-disilicate and lithia-metasilicate

Wavenumber (cm^{-1})	Quartz SiO_2 (0-NBO)	Lithia-disilicate 33L (1-NBO)	Lithia-metasilicate 50L (2-NBO)	Peak assignment
1230		X		$Si–O_2$:*X* polarized
1180	X			$Si–O_2$ (lattice)
1120			X	Si → O → Si: *Y* polarized
1115		X		Si → O → Si
1110	X			Si → O → Si
1040		X		$Si–O_{NB}$:*X* polarized
1000			X	$Si–(O_{NB})_2$:*X* polarized
995		X		$Si–O_{NB}$: *Y* polarized
965			X	$Si–(O_{NB})_2$: *Y* polarized
950		X		$Si–O_2$: *Z* polarized
870			X	$Si–O_2$: *Z* polarized

NBO: nonbridging oxygen per tetrahedron.

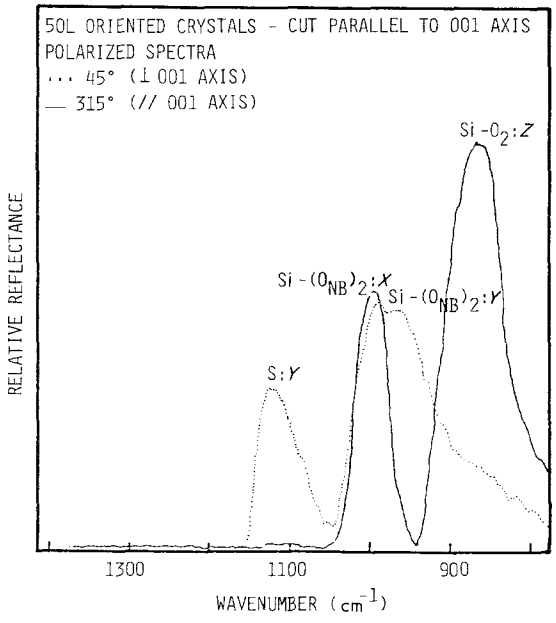

Figure 14 Polarized infrared reflection spectra of lithia-metasilicate oriented crystals on a plane parallel to the crystal growth axis (0 0 1).

seen that, by increasing the number of nonbridging oxygens per SiO_4 tetrahedra (NBO), there are two different types of frequency changes in the spectra. First, with increasing NBO, the frequency of the S type vibration and vibrations of the tetrahedral lattice increase. Secondly, vibrations involving the $Si–O_{NB}$ bonds and $Si–O_2$ bonds along tetrahedral chains decrease in frequency with increasing NBO. This shows that one cannot predict a uniform shift in spectra by changing the silicate structure.

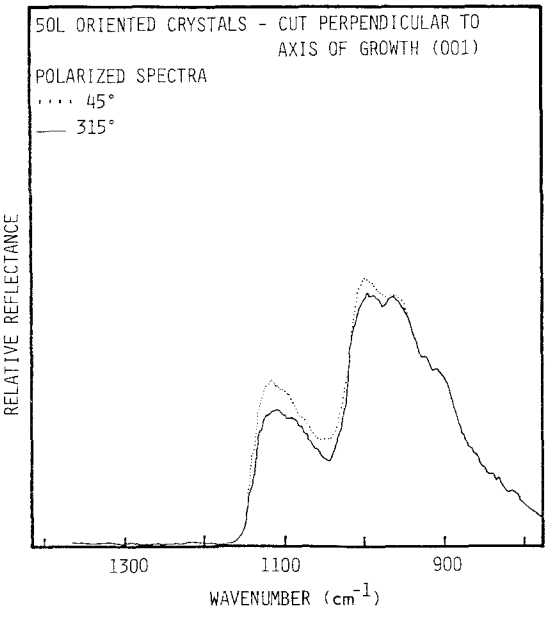

Figure 15 Polarized infrared reflection spectra of lithia-metasilicate oriented crystals on a plane perpendicular to the crystal growth axis (0 0 1).

References

1. F. MATOSII and H. BLASSCKE, *Z. Phys.* **108** (1938) 285.
2. R. J. BELL and P. DEAN, *Disc. Faraday Soc.* (1970) 55.
3. P. H. GASKELL, *ibid.* (1970) 82.
4. V. A. FLORINSKAYA and R. S. PENCHENKINA, "The Structure of Glass", Vol. 1, Translated from Russian (Consultants' Bureau, New York, 1958) p. 55.
5. F. MATOSSI, *J. Chem. Phys.* **17** (1949) 679.
6. J. REITZEL, *ibid.* **23** (1955) 2407.
7. K. J. D. MACKENZIE, *J. Amer. Ceram. Soc.* **55** (1972) 68.
8. D. M. SAUNDERS, W. B. PERSON and L. L. HENCH, *Appl. Spectrosc.* **28** (1974) 247.
9. I. SIMON, "Modern Aspects of the Vitreous Stage", Vol. 1, edited by J. D. Mackenzie (Butterworth, London, 1960) pp. 120–51.
10. V. A. KOLESOVA, *Optics and Spectroscopy* **6** (1959) 20.
11. I. SIMON and H. O. McMAHON, *Chem. Phys.* **21** (1953) 23.
12. J. BOCK and G. SU *J. Amer. Ceram. Soc.* **53** (1970) 69.
13. D. M. SAUNDERS and L. L. HENCH, *ibid.* **56** (1973) 373.
14. D. E. CLARK, M. F. KILMORE, E. C. ETHRIDGE and L. L. HENCH, *ibid.* **59** (1976) 62.
15. D. E. CLARK, E. C. ETHRIDGE, M. F. DILMORE and L. L. HENCH, *J. Glass Technol.* **18** (1977) 121.
16. D. E. CLARK, C. G. PANTANO JR and L. L. HENCH, "Corrosion of Glass" (Books for Industry, New York, 1979).
17. L. L. HENCH, *J. Non-Cryst. Solids* **19** (1975) 73.
18. R. G. GORDON, *J. Chem. Phys.* **43** (1965) 1307.
19. C. SCHAEFFER, F. MATOSSI and K. WIRTZ, *Z. Phys.* **89** (1934) 210.
20. F. MATOSSI and H. KREAGER, *ibid.* **99** (1936) 1.
21. I. SIMON, *J. Opt. Soc. Amer.* **41** (1951) 336.
22. F. A. JENKINS and H. E. WHITE, "Fundamentals of Optics", (McGraw-Hill, New York, 1957) p. 509.
23. M. BORN, and E. WOLF, "Principles of Optics" (Pergamon Press, New York, 1965).
24. D. M. SAUNDERS, PhD dissertion, University of Florida (1973).
25. J. W. ELLIS and J. BATH, *Phys. Rev.* **55** (1939) 1098.
26. J. W. GIBBS, *Proc. Roy. Soc.* **109A** (1926) 443.
27. C. FRONDEL, "The System of Mineralogy" (Wiley, New York, 1962).
28. F. LIEBAU, *Acta Crystallogr.* **14** (1961) 389.
29. F. C. KRACEK, *J. Phys. Chem.* **34** (1930) 2641.

30. G. DONNAY and J. D. H. DONNAY, *Amer. Mineral.* **38** (1953) 163.
31. G. BIRD and M. PARRISH Jr, *J. Opt. Soc. Amer.* **50** (1960) 886.
32. D. E. NEWBURY and H. YAKOWITZ, "Practical Scanning Electron Microscopy", edited by J. I. Goldstein and H. Yakowitz (1975) pp. 149–79.
33. D. G. COATES, *Phil. Mag.* **16** (1967) 1179.
34. N. B. COLTHUP, L. H. DALY and S. E. WILEY, "Introducing Infrared and Raman Spectroscopy" (Academic Press, New York, 1964).
35. E. CHARNEY, *J. Opt. Soc. Amer.* **45** (1955) 980.

Received 4 September
and accepted 13 September 1984